Earthquakes and Structures, *Vol. 14, No. 2 (2018) 129-142*
DOI: https://doi.org/10.12989/eas.2018.14.2.129

Maximum damage prediction for regular reinforced concrete frames under consecutive earthquakes

Gholamreza Ghodrati Amiri* and Elham Rajabi[a]

Center of Excellence for Fundamental Studies in Structural Engineering, School of Civil Engineering, Iran University of Science and Technology, Tehran, Iran

(Received November 7, 2016, Revised January 22, 2018, Accepted January 30, 2018)

Abstract. The current paper introduces a new approach for development of damage index to obtain the maximum damage in the reinforced concrete frames caused by as-recorded single and consecutive earthquakes. To do so, two sets of strong ground motions are selected based on maximum and approximately maximum peak ground acceleration (PGA) from "PEER" and "USGS" centers. Consecutive earthquakes in the first and second groups, not only occurred in similar directions and same stations, but also their real time gaps between successive shocks are less than 10 minutes and 10 days, respectively. In the following, a suite of six concrete moment resisting frames, including 3, 5, 7, 10, 12 and 15 stories, are designed in OpenSees software and analyzed for more than 850 times under two groups of as-recorded strong ground motion records with/without seismic sequences phenomena. The idealized multilayer artificial neural networks, with the least value of Mean Square Error (MSE) and maximum value of regression (R) between outputs and targets were then employed to generate the empirical charts and several correction equations for design utilization. To investigate the effectiveness of the proposed damage index, calibration of the new approach to existing real data (the result of Park-Ang damage index 1985), were conducted. The obtained results show good precision of the developed ANNs-based model in predicting the maximum damage of regular reinforced concrete frames.

Keywords: seismic sequence; damage index; reinforced concrete frames; empirical charts; artificial neural networks

1. Introduction

Today, many forms of damage indexes' definitions are presented in structural and earthquake engineering literature. In the majority of proposed indexes, complicated concepts such as deformation, and simple concepts such as ductility ratio and inter-story drift, as the most important factor in damage index presentation, are being used. However, energy dissipation and ductility ratio have been in the spotlight in most of these studies. Generally, the damage indexes normalize the damage on a scale of 0 to 1, where zero represents intact or undamaged state while unity represents collapse state of the building. Concrete is one of the most common building materials and cracks can be formed in the reinforced concrete elements, even before being subjected to any type of external load. In a comprehensive review, Mihai (2013) examined the damage indexes which have been used to determine the nonlinear behavior of reinforced concrete structures. In most of the studies, one of the simplest and also widely used damage indexes is the *Park and Ang* damage index, and its definition is based on the linear combination of the maximum displacement and the dissipated energy. Since then, some researchers such as Valles *et al*. (1996), Zhai *et al*. (2013), Kaveh *et al*. (2014) performed some modification on the Park and Ang index, in order to develop a new one. Recently, Guo *et al*. (2016) have extended this index to evaluate the three dimensional damage of an RC pier and Zhai *et al*. (2015) have been used Park-Ang index and the modified version of this index to report the caused structural damage by seismic scenarios.

It can be claimed that Park-Ang damage index is among of the simplest and widely used indicators in structural and earthquake engineering literature for estimating the structural damage. However, this index doesn't use directly earthquake features such as "Magnitude", "Shear Velocity" and etc. This may be more important in estimating the structural damage under given repeated shocks. Furthermore, despite the damages caused by the recent consecutive earthquakes such as Nepal and Hindu-Kush (2015), most structures are designed according to the modern seismic codes which only consider a single seismic event on the structure for analysis and design process. However, the single seismic design philosophy does not consider the effect of strong successive shocks on the accumulated damages of structures that have been already damaged by preceding shocks. Moreover, if the considered structure is located in the active seismic regions, not only it will be exposed to single seismic events, but also the risks of strong aftershocks are noticeable and should be considered. Therefore, some researchers tried to examine the effect of multiple earthquakes on the response of usual SDOF and MDOF structures and unusual cases such as

*Corresponding author, Professor
E-mail: ghodrati@iust.ac.ir
[a]Ph.D. Student
E-mail: elhamrajabi674@gmail.com

ISSN: 2092-7614 (Print), 2092-7622 (Online)

steel tower suspension bridges (Xie *et al*. 2012), ancient multidrum columns (Papaloizou *et al*. 2016) and steel arch bridges (Tang *et al*. 2016) using as-recorded and artificial models (Garcia *et al*. 2014) for repeated acceleration sequences. Since, the use of artificial seismic sequences could lead to non-conservative prediction of response and behavior of structures, in this study, a new approach is developed using multilayer artificial neural networks (ANNs) to obtain the maximum damage caused by as-recorded single and consecutive earthquakes. In order to design the ideal artificial neural networks, Park-Ang damage index is selected. It should be noted that previous researches such as Dworakowski *et al*. (2014) and Adnan and Tiong (2012) only designed the artificial neural networks to estimate the structural damage and the features of "Single" earthquakes have just been used to train the artificial neural networks in these studies. To bridge such a knowledge gap, the current paper takes into account the effects of consecutive seismic scenarios. For this reason, the empirical design charts and equations are generated in this paper using the ideal neural networks that are trained based on the features of "Single" and "Consecutive" earthquakes. In this regard, six concrete moment resisting frames with 3, 5, 7, 10, 12 and 15 stories, is designed and analyzed for more than 850 times under two different databases with/without seismic sequences phenomena. In order to determine the target values for the design of artificial neural networks, Park-Ang damage index is selected due to its extensive practical use and Simplicity. Then, idealized networks were selected based on maximum correlation and minimum error between outputs of networks and target. After determining the reference values of input nodes, the idealized networks were employed to generate the charts and equations for engineering design use. So that, proposed equations which were derived predict the maximum damage index independently from the network. In order to examine the precision of the developed ANN-based model in predicting the maximum Park-Ang damage of regular reinforced concrete frames, the results obtained from proposed equations, were verified by the results obtained from Park-Ang damage indexes generated from nonlinear dynamic analysis.

2. Selection of strong ground motions and structural modeling

In this paper, the estimation of maximum damage for reinforced concrete frames subjected to recorded earthquakes with/without sequence is considered particularly. For this purpose, single and successive strong ground motions are selected based on PGA. In this way, PGA parameter is calculated for the whole successive earthquakes which occurred in less than 10 minutes and 10 days. In each case, two databases of strong ground motions with two types of PGA are extracted. Each database involves the single and consecutive earthquakes with maximum PGA and approximately maximum PGA, that is in second or third level toward the maximum value. So, earthquakes are classified into 8 groups. Classification of earthquake databases is shown in Fig. 1. These records are available in "PEER" center. It should be noted that the recent consecutive earthquakes, such as Nepal (2015) is included in the database. The difference of databases is in their time gap (T_g) between consecutive earthquakes. In such way that, the time gap in the first database is identical to the real event (less than 10 minutes), while the seismic scenarios with sequence phenomena in the second database (occurred in less than 10 days) were made using artificial time gap, which is assumed 120 (s). This gap is enough to calm down the motion of any building due to the damping. It should be noted that in consecutive earthquakes, the acceleration during the time gap is considered to be zero. It should be noted that all of consecutive records-both of first shock and second shock in each sequence-occurred in similar directions and same stations. The ground motion features for both databases with maximum and approximately maximum PGA are listed in Tables 1-4. As shown in Fig. 1, in each database, consecutive records have two subsets: 1) first shock and second shock with maximum PGA and 2) at least one of them has maximum PGA and another is in second or third level toward the maximum value. Second subset has been named "approximately maximum PGA". This is also true for single records.

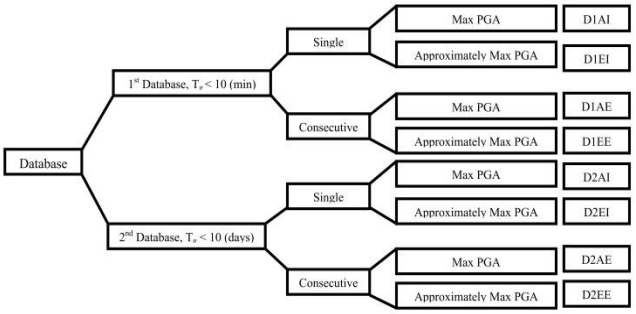

Fig. 1 Classification of the earthquake databases

Also, for compatibility aspects between the seismic analysis and seismic design (Vamvatsikos and Cornell

Table 1 The features of ground motion records in the first database with maximum PGA

Earthquake	Date	Time	Time gap (min)	Magnitude	Station	PGA
Chalfant Valley	07/21/86	14:42	9	6.19	CDMG 54428 Zack Brothers Ranch	0.4246
	07/21/86	14:51		5.65	CDMG 54428 Zack Brothers Ranch	0.1347
Hollister	04/09/61	07:23	2	5.60	USGS 1028 Hollister City Hall	0.1210
	04/09/61	07:25		5.50	USGS 1028 Hollister City Hall	0.0683
New Zealand	03/02/87	01:42	9	6.60	99999 Matahina Dam	0.2926
	03/02/87	01:51		5.80	99999 Matahina Dam	0.0525

Table 2 The features of records in the first database with approximately maximum PGA

Earthquake	Date	Time	Time gap (min)	Magnitude	Station	PGA
Chalfant Valley	07/21/86	14:42	9	6.19	CDMG 54171 Bishop - LADWP South St	0.2058
	07/21/86	14:51		5.65	CDMG 54171 Bishop - LADWP South St	0.0864
Chi- Chi Taiwan	09/20/99	17:57	6	5.90	CWB 99999 TCU079	0.3308
	09/20/99	18:03		6.20	CWB 99999 TCU079	0.3022
Imperial Valley	10/15/79	23:16	3	6.53	USGS 952 El Centro Array #5	0.4481
	10/15/79	23:19		5.01	USGS 952 El Centro Array #5	0.2374
Irpinia, Italy	11/23/80	19:34	1	6.90	ENEL 99999 Sturno	0.2898
	11/23/80	19:35		6.20	ENEL 99999 Sturno	0.0760
Northridge 1	01/17/94	12:31	1	6.69	CDMG 24279 Newhall - Fire Sta	0.6980
	01/17/94	12:32		6.05	CDMG 24279 Newhall - Fire Sta	0.0407
	01/17/94	12:41	9	5.20	CDMG, 24279 Newhall - Fire Sta	0.1632
Northridge 2	01/17/94	12:31	1	6.69	CDMG 24278 Castaic - Old Ridge Route	0.4898
	01/17/94	12:32		6.05	CDMG 24278 Castaic - Old Ridge Route	0.0231
	01/17/94	12:41	9	5.20	CDMG 24278 Castaic - Old Ridge Route	0.0389

Table 3 The features of ground motion records in the second database with maximum PGA

Earthquake	Date	Magnitude	PGA	Station
Chalfant Valley3	07/20/1986	5.77	0.2382	CDMG 54428 Zack Brothers Ranch
	07/21/1986	6.19	0.4246	CDMG 54428 Zack Brothers Ranch
Chalfant Valley4	07/20/1986	5.77	0.2382	CDMG 54428 Zack Brothers Ranch
	07/21/1986	5.65	0.1347	CDMG 54428 Zack Brothers Ranch
Coalinga	07/22/1983	4.89	0.1539	CDMG 46617 Coalinga-14th & Elm (Old CHP)
	07/25/1983	5.21	0.5813	CDMG 46617 Coalinga-14th & Elm (Old CHP)
Kalamata	09/13/1986	6.20	0.2649	ITSAK 99999 Kalamata (bsmt)
	09/15/1986	5.40	0.1869	ITSAK 99999 Kalamata (bsmt)
Kozani	05/15/1995	5.10	0.1330	ITSAK 99999 Chromio Anapsiktirio
	05/17/1995	5.30	0.1144	ITSAK 99999 Chromio Anapsiktirio
Mammoth1	05/25/1980	6.06	0.4193	CDMG 54099 Convict Creek
	05/25/1980	5.70	0.4156	CDMG 54099 Convict Creek
Mammoth2	05/25/1980	6.06	0.4193	CDMG 54099 Convict Creek
	05/26/1980	5.70	0.1234	CDMG 54099 Convict Creek
Mammoth3	01/07/1983	5.34	0.1738	CDMG 54099 Convict Creek
	01/07/1983	5.31	0.1208	CDMG 54099 Convict Creek
Mammoth4	05/27/1980	4.73	0.2178	USC 37 USC McGee Creek Inn
	05/31/1980	4.80	0.3689	USC 37 USC McGee Creek Inn
Mammoth5	05/25/1980	5.91	0.3289	CDMG 54214 Long Valley Dam (Upr L Abut)
	05/27/1980	5.94	0.6293	CDMG 54214 Long Valley Dam (Upr L Abut)
Mammoth6	05/25/1980	5.70	0.4156	CDMG 54099 Convict Creek
	05/26/1980	5.70	0.1234	CDMG 54099 Convict Creek
Managua	12/23/1972	6.24	0.3941	3501 Managua, ESSO
	12/23/1972	5.20	0.2945	3501 Managua, ESSO
Northwest1	04/05/1997	5.90	0.2437	CSB 19001 Jiashi
	04/06/1997	5.93	0.1349	CSB 19001 Jiashi
Northwest2	04/05/1997	5.90	0.2437	CSB 19001 Jiashi
	04/11/1997	6.10	0.2961	CSB 19001 Jiashi
Northwest3	04/05/1997	5.90	0.2437	CSB 19001 Jiashi
	04/15/1997	5.80	0.2091	CSB 19001 Jiashi
Northwest4	04/06/1997	5.93	0.1349	CSB 19001 Jiashi
	04/11/1997	6.10	0.2961	CSB 19001 Jiashi
Northwest5	04/06/1997	5.93	0.1349	CSB 19001 Jiashi
	04/15/1997	5.80	0.2091	CSB 19001 Jiashi
Northwest6	04/11/1997	6.10	0.2961	CSB 19001 Jiashi
	04/15/1997	5.80	0.2091	CSB 19001 Jiashi
Oroville	08/02/1975	4.79	0.0344	CDMG 1546 Up & Down Cafe (OR1)
	08/02/1975	4.37	0.0630	CDMG 1546 Up & Down Cafe (OR1)
Nepal	25/04/2015	7.8	0.164	Kanti Path, Kathmandu, Nepal
	12/05/2015	7.3	0.087	Kanti Path, Kathmandu, Nepal

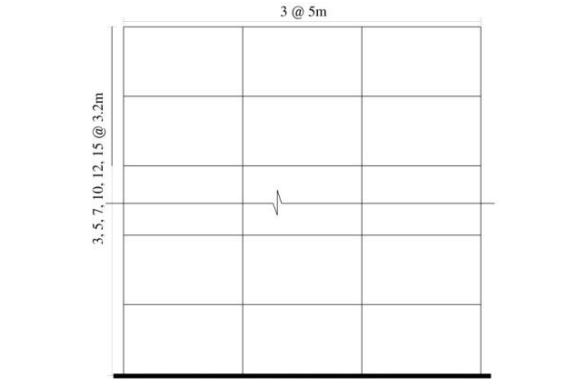

(a)

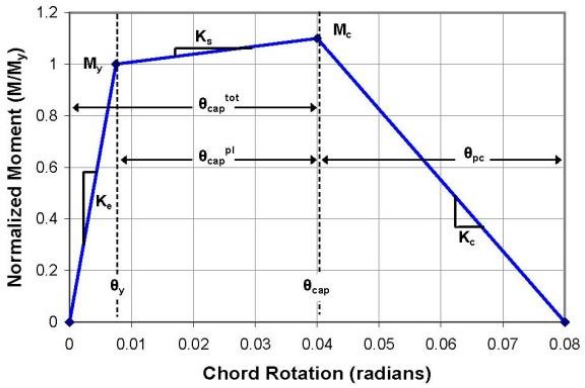

(b)

Fig. 2 The schematic of (a) the studied frames, (b) Tri-linear backbone curve suggested by Ibarra (Haselton *et al*. 2007)

2002), the aforementioned seismic events have been appropriately scaled to have identical spectral acceleration with the design spectrum for the fundamental period of each structure. In this regard, linear scaling (Atkinson 2009) is used to scale all ground motion records by multiplying time histories by the appropriate factor (Hancock *et al*. 2008). The mentioned technique is convenient for implementation. Also, the frequency content and original phasing of the records are preserved in this method (Atkinson 2009). A set of 2-D concrete intermediate moment resisting frames under vertically regular condition (stiffness and strength) with 3, 5, 7, 10, 12 and 15 stories is designed according to ASCE7-05 and analyzed in OpenSEES software. In addition, this software can use different elements for modeling of structural and non-structural sections. Moreover, equivalent lateral design forces were determined based on ASCE7-05 standard, i.e., the design spectrum was derived, and the corresponding design base shears were calculated, then both gravity and seismic loads were imposed on the frames according to the counteractive load combinations of this standard (the reader is referred to Section 12.4.2.3 of ASCE7-05 for further details).

The schematic elevation of the considered concrete frames and tri-linear backbone curve for beam elements suggested by Ibarra (Haselton *et al*. 2007) is shown in Fig. 2. The story height and the bay lengths are 500 and 320 cm, respectively. The geometric and material properties of the designed 3, 5, 7, 10, 12 and 15 story frames are presented in Tables 5-6. In this paper, the nonlinear beams with concentrated plastic hinges and columns with fiber section are employed to simulate the nonlinear flexural behavior of the moment frames. In this regard, the "beam with hinges element" is chosen for modeling of the beams and a predetermined length at both ends was allocated to the plastic hinges, and an elastic material was assigned to the mid span. Therefore, the coefficient of cracking was set to be 0.5 for the elastic segment of the beams.

As the nonlinear behavior was assumed to be focused in the hinges, expansion of the non-linearity to the elastic region was less likely to happen. The nonlinear behavior of the plastic hinges was defined in accordance with Haselton *et al.* (2007) which proposes essential relationships for RC members, based on the calibration of numerous test results in the form of the tri-linear backbone curve suggested by Ibarra (Fig. 2(b)). In concrete models, important features such as (1) softening due to concrete crushing, reinforcement buckling, (2) yielding and (3) bond slip can be considered in the negative stiffness region of proposed backbone curve, namely the post cap behavior. Specifications of this model have been calibrated using the results of empirical tests on a large number of beam-columns involved 306 rectangular and 177 circular columns, which extracted from PEER Structural Performance center.

Finally, parameters of this model were calibrated according to the result of 255 experimental tests on RC columns. Four modes of deterioration is illustrated in this model: (1) Accelerated reloading stiffness deterioration, (2) Unloading stiffness deterioration, (3) strength deterioration of nonlinear strain hardening branch and (4) Post-cap strength deterioration of strain softening. More details such as computational equations related to the required parameters are available in Haselton *et al*. (2007). Thus, reinforced concrete frames behave according to the backbone curve under seismic scenarios and pass the linear region and make hysteresis loops. On the other hands, strength deterioration has been considered by tri-linear backbone curve suggested by Ibarra and the hysteresis energy absorbed during the earthquake – as one of most important parameters of Park-Ang (1985) damage index – can be calculated by the area under these hysteresis loops. The tri-linear Ibarra model, as mentioned above, was employed in the OpenSEES platform using the Clough material proposed by Altoontash (Haselton *et al*. 2007). Columns were modeled by means of the fiber method with the capability of developing distributed plasticity along the entire length of the element. This choice was made mostly due to the fact that the flexural behavior in the columns is highly dependent on the interaction of their axial and bending forces. Reinforced concrete frames are verified by the analytical and experimental result obtained from a parametric study and a test of structure on shaking table. In the first phase, the results of Huang *et al*. (2014) are used and for the next phase, the studied reinforced concrete frames are verified according to results of Nagae *et al*., (2015), which in their study, a full scale reinforced concrete building – 4 story – was tested on the E-Defense shake table that is provided by E-Defense – National Research Institute for Earth Science and Disaster Prevention (NIED) – company in Japan Nagae *et al*. (2015).

Table 4 The features of records in the second database with approximately maximum PGA

Earthquake	Date	Magnitude	PGA	Station
Chalfant Valley5	07/21/1986	6.19	0.4246	CDMG 54428 Zack Brothers Ranch
	07/31/1986	5.44	0.0616	CDMG 54428 Zack Brothers Ranch
Chalfant Valley6	07/21/1986	5.65	0.1347	CDMG 54428 Zack Brothers Ranch
	07/31/1986	5.44	0.0616	CDMG 54428 Zack Brothers Ranch
Chalfant Valley7	07/21/1986	6.19	0.2058	CDMG 54171 Bishop - LADWP South St
	07/31/1986	5.44	0.1515	CDMG 54171 Bishop - LADWP South St
Chalfant Valley8	07/21/1986	5.65	0.0864	CDMG 54171 Bishop - LADWP South St
	07/31/1986	5.44	0.1515	CDMG 54171 Bishop - LADWP South St
Chalfant Valley9	07/20/1986	5.77	0.1105	CDMG 54171 Bishop - LADWP South St
	07/21/1986	6.19	0.2058	CDMG 54171 Bishop - LADWP South St
Chalfant Valley10	07/20/1986	5.77	0.1105	CDMG 54171 Bishop - LADWP South St
	07/21/1986	5.65	0.0864	CDMG 54171 Bishop - LADWP South St
Coalinga1	07/22/1983	5.77	0.4543	CDMG 46617 Coalinga-14th & Elm (Old CHP)
	07/22/1983	4.89	0.1539	CDMG 46617 Coalinga-14th & Elm (Old CHP)
Coalinga2	07/22/1983	5.77	0.4543	CDMG 46617 Coalinga-14th & Elm (Old CHP)
	07/25/1983	5.21	0.5813	CDMG 46617 Coalinga-14th & Elm (Old CHP)
Coalinga3	07/22/1983	4.89	0.0395	CDMG 47T03 Sulphur Baths (temp)
	07/25/1983	5.21	0.2053	CDMG 47T03 Sulphur Baths (temp)
Kalamata	09/13/1986	6.20	0.2649	ITSAK 99999 Kalamata (bsmt)
	09/15/1986	5.40	0.1767	ITSAK 99999 Kalamata (bsmt)
Kozani1	05/15/1995	5.10	0.0407	ITSAK 99999 Grevena
	05/17/1995	5.30	0.0242	ITSAK 99999 Grevena
Kozani2	05/15/1995	5.10	0.0407	ITSAK 99999 Grevena
	05/19/1995	5.10	0.0316	ITSAK 99999 Grevena
Kozani3	05/17/1995	5.30	0.0242	ITSAK 99999 Grevena
	05/19/1995	5.10	0.0316	ITSAK 99999 Grevena
Livermore	01/24/1980	5.80	0.1066	CDMG 57187 San Ramon - Eastman Kodak
	01/27/1980	5.42	0.1917	CDMG 57187 San Ramon - Eastman Kodak
Mammoth1	05/25/1980	6.06	0.4193	CDMG 54099 Convict Creek
	05/25/1980	5.69	0.1669	CDMG 54099 Convict Creek
Mammoth2	05/25/1980	6.06	0.4193	CDMG 54099 Convict Creek
	05/25/1980	5.91	0.2172	CDMG 54099 Convict Creek
Mammoth3	05/25/1980	5.91	0.3289	CDMG 54214 Long Valley Dam (Upr L Abut)
	05/25/1980	5.70	0.2403	CDMG 54214 Long Valley Dam (Upr L Abut)
Mammoth4	05/25/1980	5.91	0.3289	CDMG 54214 Long Valley Dam (Upr L Abut)
	05/26/1980	5.70	0.0926	CDMG 54214 Long Valley Dam (Upr L Abut)
Mammoth5	05/25/1980	6.06	0.2818	CDMG 54301 Mammoth Lakes H. S.
	05/25/1980	5.69	0.4143	CDMG 54301 Mammoth Lakes H. S.
Mammoth6	05/25/1980	5.69	0.1369	CDMG 54214 Long Valley Dam (Upr L Abut)
	05/25/1980	5.91	0.3289	CDMG 54214 Long Valley Dam (Upr L Abut)
Mammoth7	05/25/1980	6.06	0.3403	CDMG 54214 Long Valley Dam (Upr L Abut)
	05/25/1980	5.91	0.3289	CDMG 54214 Long Valley Dam (Upr L Abut)
Mammoth8	05/25/1980	6.06	0.3403	CDMG 54214 Long Valley Dam (Upr L Abut)
	05/27/1980	5.94	0.6293	CDMG 54214 Long Valley Dam (Upr L Abut)
Mammoth9	05/26/1980	5.70	0.0926	CDMG 54214 Long Valley Dam (Upr L Abut)
	05/27/1980	5.94	0.6293	CDMG 54214 Long Valley Dam (Upr L Abut)
Mammoth10	05/25/1980	5.70	0.2403	CDMG 54214 Long Valley Dam (Upr L Abut)
	05/27/1980	5.94	0.6293	CDMG 54214 Long Valley Dam (Upr L Abut)

3. Damage Index

Park and Ang's damage index (1985) is a well-known damage indexes which has been widely used in practice.

It is based on scaled values of ductility and dissipated energy of the local element during the seismic ground shaking. The damage index (DI) is defined as a combination of maximum deformation and hysteresis energy

$$DI = \frac{\delta_m}{\delta_u} + \frac{\beta}{P_y \delta_u} \int dE_h \tag{1}$$

Table 4 Continued

Earthquake	Date	Magnitude	PGA	Station
Mammoth11	05/25/1980	6.06	0.3403	CDMG 54214 Long Valley Dam (Upr L Abut)
	05/27/1980	5.94	0.6293	CDMG 54214 Long Valley Dam (Upr L Abut)
Mammoth12	05/25/1980	5.91	0.2172	CDMG 54099 Convict Creek
	05/25/1980	5.70	0.4156	CDMG 54099 Convict Creek
Mammoth13	05/25/1980	5.69	0.1669	CDMG 54099 Convict Creek
	05/25/1980	5.70	0.4156	CDMG 54099 Convict Creek
Mammoth14	05/25/1980	5.91	0.2172	CDMG 54099 Convict Creek
	05/26/1980	5.70	0.1234	CDMG 54099 Convict Creek
Mammoth15	05/25/1980	5.69	0.1669	CDMG 54099 Convict Creek
	05/26/1980	5.70	0.1234	CDMG 54099 Convict Creek
Mammoth16	05/25/1980	6.06	0.3403	CDMG 54214 Long Valley Dam (Upr L Abut)
	05/25/1980	5.70	0.2403	CDMG 54214 Long Valley Dam (Upr L Abut)
Mammoth17	05/25/1980	6.06	0.3403	CDMG 54214 Long Valley Dam (Upr L Abut)
	05/26/1980	5.70	0.0926	CDMG 54214 Long Valley Dam (Upr L Abut)
Mammoth18	05/25/1980	5.70	0.2403	CDMG 54214 Long Valley Dam (Upr L Abut)
	05/26/1980	5.70	0.0926	CDMG 54214 Long Valley Dam (Upr L Abut)
Mammoth19	05/25/1980	5.69	0.1669	CDMG 54099 Convict Creek
	05/25/1980	5.91	0.2172	CDMG 54099 Convict Creek
Northwest7	04/05/1997	5.90	0.0392	CSB 19002 Xiker
	04/06/1997	5.93	0.0748	CSB 19002 Xiker
Northwest8	04/05/1997	5.90	0.0392	CSB 19002 Xiker
	04/11/1997	6.10		CSB 19002 Xiker
Northwest9	04/05/1997	5.90	0.0392	CSB 19002 Xiker
	4/15/1997	5.80	0.0997	CSB 19002 Xiker
Northwest10	04/06/1997	5.93	0.0748	CSB 19002 Xiker
	04/11/1997	6.10		CSB 19002 Xiker
Northwest11	04/06/1997	5.93	0.0748	CSB 19002 Xiker
	04/15/1997	5.80	0.0997	CSB 19002 Xiker
Northwest12	04/11/1997	6.10		CSB 19002 Xiker
	04/15/1997	5.80	0.0997	CSB 19002 Xiker
Northridge	01/17/1994	5.93	0.122	CDMG 24278 Castaic - Old Ridge Route
	01/17/1994	5.13	0.081	CDMG 24278 Castaic - Old Ridge Route
Oroville	08/02/1975	4.79	0.0274	CIT 1545 Oroville Airport
	08/02/1975	4.37	0.0229	CIT 1545 Oroville Airport
Nepal	25/04/2015	7.8	0.164	Kanti Path, Kathmandu, Nepal
	12/05/2015	6.7	0.065	Kanti Path, Kathmandu, Nepal

Table 5 Geometric properties of the designed 3, 5, 7, 10, 12 and 15 story frames

Number Of story	Level	Column Width (cm)	Column Height (cm)	Beam Width (Cm)	Beam Height (cm)
3	1, 2, 3	40	40	40	35
5	1, 2	50	50	50	40
	3, 4, 5	40	40	50	40
7	1, 2, 3, 4	55	55	55	45
	5, 6, 7	45	45	45	35
10	1, 2, 3, 4	55	55	55	40
	5, 6, 7	45	45	45	40
	8, 9, 10	40	40	40	35
12	1, 2, 3, 4	60	60	60	50
	5, 6, 7, 8	55	55	55	40
	9, 10, 11, 12	40	40	40	35
15	1, 2, 3, 4	65	65	65	50
	5, 6, 7, 8	55	55	55	50
	9, 10, 11, 12	45	45	45	40
	13, 14, 15	35	35	35	35

Table 6 Material properties of the designed 3, 5, 7, 10, 12 and 15 story frames (kg/cm^2)

Specified Concrete Compression Strength	Modulus of Elasticity	Yield Stress
250	2.388 e+5	4000

Where δ_m is the maximum deformation of the element, δ_u represents the ultimate deformation, β is a model constant parameter, usually considered 0.05-0.20, to control strength deterioration, $\int dE$, the hysteresis energy absorbed by the element during the earthquake and P_y is the yield strength of the element. In order to calculate the Damage index –based on Eq. (1) -β is taken as 0.15 according to Park *et al*. (1987) for nominal strength deterioration. In order to calculate this damage index, the control node is selected at the center of mass at the roof of each RC frame. The target displacement at each floor level has been calculated in accordance with Eqs. (3)-(15) of FEMA 356 (the reader would be referred to Section 3.3.3.3.2 of FEMA

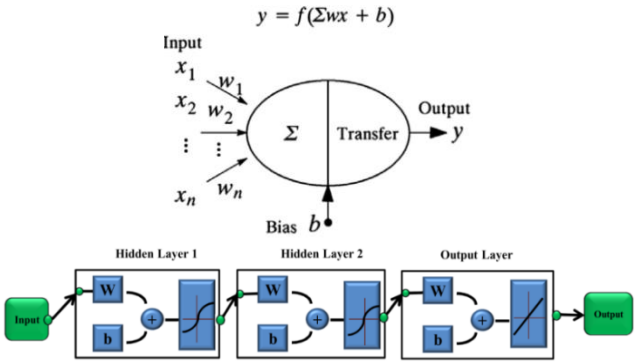

Fig. 3 Schematic of computational neuron components (Hagan 2014) and studied artificial neural networks

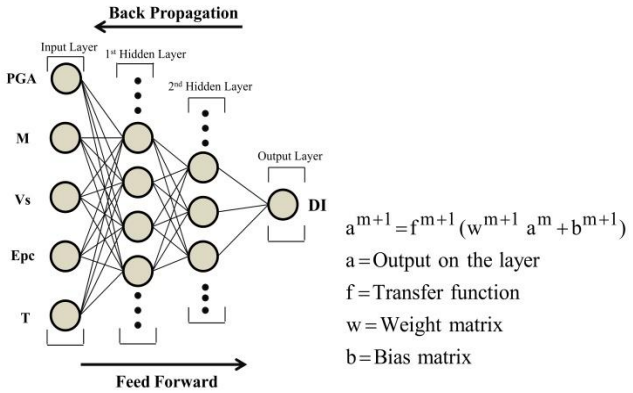

Fig. 4 Schematic of back propagation algorithm in neural network of single earthquakes

356 for further details).

A uniform distribution consisting of lateral forces at each level proportional to the total mass at each level is selected and nonlinear static analysis (Push over analysis) has been done. The ultimate displacement and yield strength can be determined based on force-displacement relation between base shear and displacement of control node. Moreover, maximum displacement and hysteresis energy absorbed during the earthquake determine based on the nonlinear dynamic analysis result of RC frames under single and consecutive earthquakes.

4. Artificial neural networks

From the mathematical point of view, the neural network is a "vector mapper" that maps an input vector to an output vector. With known combinations of input and target data, the neural network can be "trained" to extract the underlying characteristics and relationships from the data (Leung *et al*. 2006). Perhaps, it can be said that artificial neural networks have been used for more than 60 years ago when McCulloch and Pitts founded the neural networks by proposing a mathematical model in 1943 (McCulloch *et al*. 1943). Artificial neural networks are highly nonlinear and can capture the complex interactions among input/output variables in a system without any prior knowledge about the nature of these interactions. These networks do not involve complicated derivations; however, they are able to analyze problems involving a large number of variables (Leung *et al*. 2006). It seems that artificial neural networks are considered as a powerful regression tool and their main advantages are high abilities and simplicity in use. In civil engineering, neural networks have been applied to various aspects, such as structural analysis and design (Hajela and Berke 1991), structural damage assessment (El-Kordy *et al*. 1993), structural control (Chen *et al*. 1995) and etc. Neural networks are made up of simple elements called neurons that operate in parallel. A schematic drawing of a simplified computational neuron and studied neural networks is shown in Fig. 3.

Each neuron can receive an input vector (x_i) and perform a series of mathematical operations, including the calculation of a weighted sum $W_i\ x_i+b$ (where b is the bias) and can produce a unique output value (y) through a transfer function (Hagan 2014). As mentioned earlier, the damage of reinforced concrete structure under single and consecutive earthquakes is estimated by multilayer neural networks (Fig. 3) with back-propagation learning algorithm. This algorithm is the generalization of the Widrow-Hoff learning rule to multiple layer networks and nonlinear differentiable transfer functions and employed for modifying the weights and biases of the network. Since networks have biases, the sigmoid layers and a linear output layer are capable of approximating any function with a finite number of discontinuities, input vectors and the corresponding target vectors are used to train a network until it can find the relationship between inputs and target, classify the inputs and approximate a function for them (Hagan 2014). Standard back propagation is a gradient descent algorithm (Fig. 4), which the randomly network weights moved along the negative of the gradient of the performance function. After the calculation of output at each step (obtained ($W_i\ x_i+b$) that has passed from the transfer function: $f(W_i\ x_i+b)$), the weights are corrected according to the difference between the targets and outputs until the error (i.e., the difference between the predicted value of the network and the actual value of the Park-Ang damage index) has been minimized. In back propagation algorithm, excitation function of each neuron is equal to the weighted sum of its input. In the next step, the minimization is performed with Levenberg-Marquardt algorithm which used for least squares problems. This algorithm is a modified steepest descent approach and a combination of Newton-Gauss methods that adjusts the slope of descent with a scalar parameter to achieve more rapid convergence. Also, input vectors and target vectors were divided into three sets including training, validation and testing (Hagan 2014). Here, the values of 60%, 35%, and 5% were randomly selected for training, testing and validation respectively in order to obtain the most efficient distribution sets of data and prevent the over fitting issue. So, 60% of whole data was specified as the training data in which the network would be adjusted according to its error. Similarly, 5% of the database was considered as the validating data which was used to measure network generalization and to halt training when generalization stops improving.

Table 7 Statistical properties of data in 1st database 1-Maximum PGA

Database	Input nodes	Minimum	Maximum	Mean	Standard deviation	Coefficient of variation
D1AI	PGA	0.121	0.4246	0.28	0.1279	0.46
	M	5.6	6.6	6.13	0.4223	0.07
	V_s (m/s)	198.8	424.8	298.3	96.94	0.325
	Epc (Km)	14.33	24.23	19.72	4.21	0.214
	T (s)	0.863	3.175	1.82	0.84	0.463
	DI	0.04	2.78	0.78	0.75	0.96
D1AE	PGAa/PGAm	0.179	0.564	0.354	0.164	0.464
	Ma/Mm	0.879	1	0.93	0.053	0.056
	V_s (m/s)	198.8	424.8	298.3	96.94	0.325
	Epca/Epcm	0.918	1.108	1.03	0.084	0.081
	T_g (min)	2	9	6.67	3.4	0.51
	T (s)	0.863	3.175	1.82	0.84	0.463
	DI	0.121	4.43	1.88	1.31	0.7

Table 8 Statistical properties of data in 1st database-Approximately Maximum PGA

Database	Input nodes	Minimum	Maximum	Mean	Standard deviation	Coefficient of variation
D1EI	PGA	0.2058	0.698	0.41	0.162	0.395
	M	5.9	6.9	6.48	0.343	0.053
	V_s (m/s)	205.6	1000	426.73	271.82	0.637
	Epc (Km)	16.24	40.68	25.94	8.26	0.32
	T (s)	0.863	3.175	1.82	0.84	0.463
	DI	0.002	4.55	1.8	1.33	0.74
D1EE	PGAa/PGAm	0.047	0.914	0.372	0.304	0.82
	Ma/Mm	0.767	1.051	0.906	0.083	0.092
	V_s (m/s)	205.6	1000	426.73	271.82	0.637
	Epc_a/Epc_m	0.343	1.278	0.727	0.33	0.452
	T_g (min)	1	9	3.5	3.08	0.88
	T (s)	0.86	3.18	1.82	0.84	0.46
	DI	0.005	8.9	2.33	1.75	0.75

Finally the remaining 35% of whole data was specified as the testing data which has no effects on training and provides an independent measure of network performance during and after the training process. The selected criterion to stop the training process of the networks was Mean Square Error (MSE) which is the average squared difference between outputs and targets. Lower values mean better performance of the network (zero value means no error). Furthermore, the regression values (*R*-values) measure the correlation between outputs and targets in the networks. *R*-value of 1 means a close relationship, while the value of 0 indicates a random relationship. These two criteria (MSE and *R*-values) were considered as the basis for selecting the idealized network.

4.1 Neural network modeling

In order to achieve a suitable model of neural network, providing homogeneous and sufficient information for training, verifying and testing of neural networks is essential. So, as mentioned earlier in the first step, to estimate the structural damage under earthquakes with/without seismic sequence phenomena, eight comprehensive sets of data were collected.

The selected databases contain period of structures (T) and some of the earthquake features including PGA, magnitude (M), shear wave velocity at the station (V_s), epicentral distance (Epc) and time gap between consecutive earthquakes (T_g) as artificial neural network inputs and Damage index (DI) based on Park-Ang damage index, as a target. It should be noted that the time gap between the first and second shocks is just for consecutive earthquakes with real delay in the first database. However, the ratio of parameters in the second shake to first one – except the shear wave velocity at the station. Because, both stations are same – are used to reduce the number of neural network inputs for consecutive earthquakes. Also, the structural damage as the results of nonlinear dynamic analysis in OpenSees software is neural network targets. As mentioned previously, structural damage under single and multiple earthquakes is calculated according to Eq. (1) by Park-Ang damage index. For this, at the beginning, the first shock is applied to the frames and damage index is calculated. Then, the time gap-with zero acceleration-is set between shocks and with applying the consecutive earthquakes, damage index is calculated for the consecutive case. The Statistical properties of inputs and targets are listed in Tables 7-10 for each case. In the network architectures "D" means Database, 1 and 2 are database number, -in database 1 and 2, the time gap between consecutive earthquakes is real and 120 (s) -"A" and "E" mean "Maximum PGA" and "approximately Maximum PGA" respectively, "I" and "E" mean "Single" and "Consecutive" earthquake respectively. As shown in Fig. 1 D2AE means consecutive earthquakes

Table 9 Statistical properties of data in 2nd database-Maximum PGA

Database	Input nodes	Minimum	Maximum	Mean	Standard deviation	Coefficient of variation
D2AI	PGA	0.0344	0.4193	0.241	0.111	0.46
	M	4.73	7.8	5.76	0.745	0.13
	V_s (m/s)	271.4	600	342.47	81.04	0.237
	Epc (Km)	1.33	59.9	13.47	13.47	13.77
	T (s)	0.863	3.175	1.82	0.84	0.463
	DI	0.0001	3.72	0.51	0.8	1.85
D2AE	PGAa/PGAm	0.294	3.777	1.188	0.821	0.691
	Ma/Mm	0.833	1.073	0.979	0.06	0.062
	V_s (m/s)	271.4	600	328.53	75.3	0.23
	Epca/Epcm	0.714	6.545	1.605	1.28	0.798
	T (s)	0.863	3.175	1.82	0.84	0.463
	DI	0	6.94	1.24	1.67	1.35

Table 10 Statistical properties of data in 2nd database-approximately Maximum PGA

Database	Input nodes	Minimum	Maximum	Mean	Standard deviation	Coefficient of variation
D2EI	PGA	0.024	0.454	0.178	0.128	0.72
	M	4.79	7.8	5.84	0.538	0.092
	V_s (m/s)	271.4	617.4	347	89.57	0.258
	Epc (Km)	1.43	81.09	23.27	18.43	0.79
	T (s)	0.863	3.175	1.82	0.84	0.463
	DI	0	3.46	0.37	0.69	1.82
D2EE	PGAa/PGAm	0.145	6.796	1.381	1.26	0.91
	Ma/Mm	0.847	1.073	0.968	0.057	0.059
	V_s (m/s)	271.4	617.4	338.66	73.55	0.217
	Epca/Epcm	0.32	6.014	1.169	0.99	0.85
	T (s)	0.863	3.175	1.8201667	0.84	0.463
	DI	0	8.45	1.04	1.52	1.465

Table 11 Scaling equations of input and target nodes

Scaling equation	Parameter
i	$i_{Scaled} = 0.1 + (0.9-0.1)(i - i_{\min}) / (i_{\max} - i_{\min})$

with the maximum PGA in the second database. Since two hidden layers with sigmoid transfer functions are used in all of the artificial neural network modellings, to ensure more suitable performance of this function, normalization/ scaling of the whole data is made before training the selected data. This has been done since the sigmoid transfer function is used in the network, which recognizes values between 0 and 1. In order to scale the data from 0.1 to 0.9 (According to Table 11), minimum and maximum values were taken using a linear relationship between those values (Leung *et al*. 2006). After entering the normalized inputs and targets data to neural networks, they are trained until the error is minimized and then, the outputs are obtained. As previously mentioned, in this paper two hidden layers are used in all of the networks. In order to achieve the ideal neural network for the both databases, 400 networks are designed with a different number of hidden neurons in each layer from 1 to 20. Then idealized neural networks are selected with the least value of MSE and maximum value of *R* among all networks. For example, the regression values of two networks – regarding the first database in single and consecutive cases with maximum PGA – with different

Table 12 Optimal neuron's number in idealized neural networks

Databse	Neural Network	1st hidden layer	2nd hidden layer
1st Database	D1AI	4	17
	D1AE	16	11
	D1EI	17	12
	D1EE	20	5
2nd Database	D2AI	6	17
	D2AE	6	19
	D2EI	10	16
	D2EE	10	19

number of hidden nodes in each layer are presented in Fig. 5. In this figure, maximum Regression values are shown by Solid circle. In this way, the number of hidden nodes in each layer of idealized networks (Table 12) is determined according to maximum *R* value. It should be noted that in the neural network fitting process, the choice of neuron numbers is an important matter. With too few neurons, the network will not be able to fit the data well. However, with too many neurons, "over fitting" may occur (Leung *et al*. 2006). For example, the mean squared error of networks for consecutive earthquakes in the first database is shown in Fig. 6. The curves have three lines, because the input and target vectors are randomly divided into three sets. In all

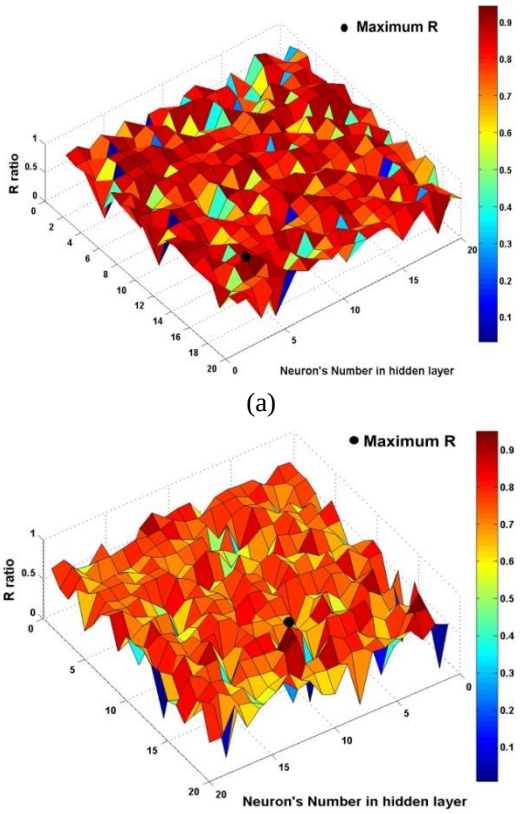

Fig. 5 Regression values between target and output of neural networks, 1st database, (a) Single earthquakes with maximum PGA, (b) Consecutive earthquakes with maximum PGA

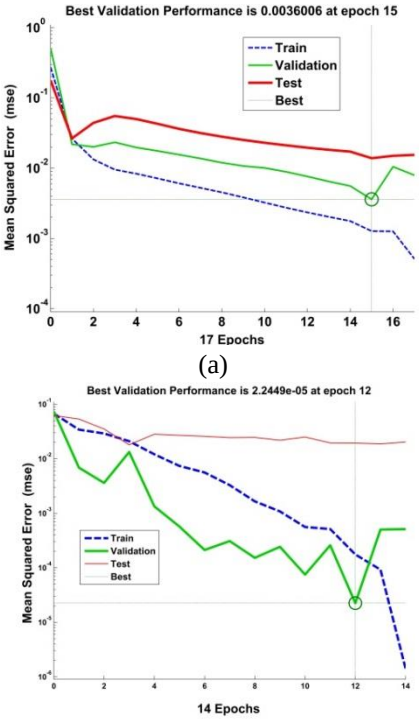

Fig. 6 Performance of neural networks for consecutive earthquakes in 1st database, (a) Maximum PGA, (b) Approximately maximum PGA

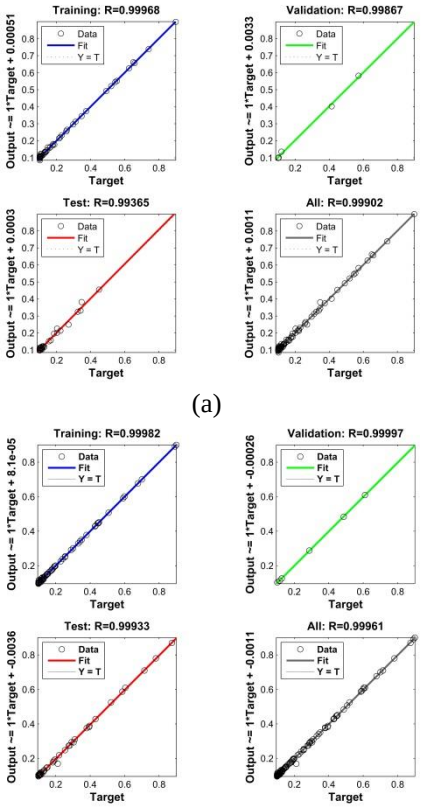

Fig. 7 Simulated regression values by neural networks in training, validation and test stage – 2nd database, (a) Single earthquakes with maximum PGA, (b) Consecutive earthquakes with maximum PGA

cases, the curves have been started at a large value and decreased to a smaller one. In other words, these figures show that the networks have well learned. Training on the vectors continues as long as the network's errors on the validation vectors are reduced.

Then, the networks memorize the training set (at the expense of generalizing more poorly), and the training is stopped automatically. The values of mean square error and corresponding epoch have been shown in Fig. 6 for 2 cases. Simulated regression values by neural networks in the training process, the validation and test stages (for second database, Maximum PGA) are shown in Fig. 7. As can be seen in this figure, the correlation between targets and outputs of neural networks is close to one.

5. Development of the empirical approach to determine the maximum damage of reinforced concrete structures under single and consecutive earthquakes

As it was indicated in the previous section, the simulated results from the neural networks for both databases in single and consecutive cases with maximum PGA and approximately maximum PGA are in reasonably good agreement with the target data. But it is not convenient to use the networks in engineering design. Since

Table 13 Range of input parameters and their corresponding reference values used in derivation of empirical design approach-single earthquake

Database	Input parameters				
	PGA	M	V_s (m/s)	Epc (Km)	T (s)
D1AI	0.29	6	270	20	1.7
D1EI	0.39	6.525	318	24	1.7
D2AI	0.24	5.9	340	11	1.7
D2EI	0.145	5.785	338	16	1.7

Table 14 Range of input parameters and their corresponding reference values used in derivation of empirical design approach-Consecutive earthquake

Database	Input parameters				
	PGAa/PGAm	Ma/Mm	V_s (m/s)	Epca/Epcm	T (s)
D1AE	0.29	6	270	20	8.6
D1EE	0.39	6.525	318	24	3
D2AE	0.24	5.9	340	11	
D2EE	0.145	5.785	338	16	

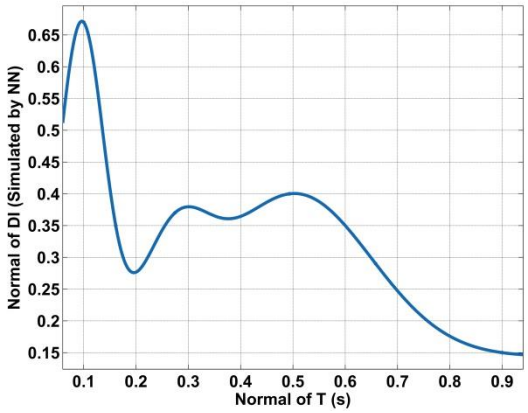

Fig. 8 Variations of "DI" at reference parametric values, Single earthquakes with maximum PGA in 1st database

the network contains many weights and biases with transfer functions, the final equations will become very complicated. In order to solve with this problem, the neural networks should be employed to generate empirical design charts and equations for use in the design process. To come up with an empirical design approach, the range and reference values for each group of input parameters such as period of RC frames "T"– for both databases in single and consecutive cases with maximum PGA and approximately maximum PGA – are defined in Tables 13-14.

The reference values of each parameter are chosen to be close to the median values. The pattern formula used for predicting the maximum damage of reinforced concrete structures under single and consecutive earthquakes in the first and second databases is the same. For this reason, the steps are described in details just for single earthquakes in the first database with maximum PGA case as follows: In the first step, "DI" parameter is plotted against period of RC frames "T" in Fig. 8 and Eq. (2) with assuming the other input parameters are kept constant at their respective reference values. To account the effect of these parameters on DI, a correction function has to be derived. This function can be written in Eq. (3).

According to Eq. (3), the variation of "DI" with each parameter is assumed to be independent of the other parameters. To illustrate that this assumption is acceptable, the correction factor C(PGA) will be derived as an example. To derive C(PGA), master curves are first obtained with different "M" values, but with "PGA" fixed at the normal reference value. For each combination of "PGA" and "M", "DI" is obtained from the neural network. By dividing the network simulated values by the results derived from the master curves, the correction factor C(PGA) can be obtained.

The same process was performed to plot C(PGA) against variations of other input parameters including "V_s" and "Epc". By considering all curves for C(PGA) that are shown in Fig. 9, a curve that fits the others with the minimum least square error was found according to Eq. (4). The same procedure has been applied to obtain the correction factors for the other input parameters, C(M), C(V_s) and C(Epc). These factors are shown in Eqs. (5)-(7). Consequently, the normalized maximum damage of reinforced concrete structure under single earthquake with the maximum PGA in first database is obtained from Eq. (8).

$$DI(T) = 0.157\ e^{-\left(\frac{T-3.786}{9.58}\right)^2} + 0.1558\ e^{-\left(\frac{T-0.273}{0.09165}\right)^2} + 0.527\ e^{-\left(\frac{T-0.0955}{0.0604}\right)^2} + 0.261\ e^{-\left(\frac{T-0.503}{0.207}\right)^2} \quad (2)$$

$$F(PGA, M, V_s, Epc) = C(PGA) \times C(M) \times C(V_s) \times C(Epc) \quad (3)$$

$$C(PGA) = -1.4\,PGA^5 + 7.49\,PGA^4 - 15.2\,PGA^3 + 14.52\,PGA^2 - 5.6\,PGA + 1.193 \quad (4)$$

$$C(M) = 1.573\ e^{-\left(\frac{M-2.13}{0.564}\right)^2} + 0.224\ e^{-\left(\frac{M-1.375}{0.396}\right)^2} + 0.92\ e^{-\left(\frac{M-0.305}{1.862}\right)^2} \quad (5)$$

$$C(Epc) = 0.57\,Epc^4 - 1.93\,Epc^3 + 2.48\,Epc^2 - 0.98\,Epc + 0.86 \quad (6)$$

$$C(V_s) = 1.058 - 0.424\cos(\omega V_s) - 0.19\sin(\omega V_s) - 0.051\cos(2\omega V_s) - 0.045\sin(2\omega V_s) - 0.068\cos(3\omega V_s) - 0.056\sin(3\omega V_s),\quad \omega = 1.644 \quad (7)$$

$$DI = DI(T) \times C(PGA) \times C(M) \times C(V_s) \times C(Epc) \quad (8)$$

Finally, damage index is calculated according to DI equation in Table 11 and Minimum and maximum values in Table 7. In other cases, determination of maximum damage approach in reinforced concrete structures is similar to above manner. For example, proposed equations for

Table 18 Proposed approach - consecutive earthquakes with approximately maximum PGA in 2nd database

$DI(T)$	$0.557\ e^{-\left(\frac{T-0.1}{0.047}\right)^2} + 0.282\ e^{-\left(\frac{T-0.27}{0.066}\right)^2} + 0.392\ e^{-\left(\frac{T-0.534}{0.0465}\right)^2} + 0.11\ e^{-\left(\frac{T-0.754}{0.332}\right)^2}$
$C(PGA)$	$\begin{cases} 1.31\sin(0.7\,PGA+0.228)+0.7\sin(8.456\,PGA-3.79)+0.66\sin(8.92\,PGA-1.1) \\ +0.0195\sin(16.69\,PGA-0.675) \quad for\ PGA \le 1.88 \\ 3.62\sin(1.14\,PGA-2.18)+1.566\sin(1.926\,PGA-1.265) \quad for\ PGA > 1.88 \end{cases}$
$C(M)$	$\begin{cases} 1.556\ e^{-\left(\frac{M-0.38}{0.045}\right)^2} + 1.83\ e^{-\left(\frac{M-0.2}{0.1024}\right)^2} + 1.26\ e^{-\left(\frac{M-0.571}{0.268}\right)^2} + 41.66\ e^{-\left(\frac{M-1.954}{0.58}\right)^2} \quad for\ M \le 0.8 \\ 2.67\ e^{-\left(\frac{M-1.65}{0.138}\right)^2} + 1.443\ e^{-\left(\frac{M-0.85}{0.194}\right)^2} + 0.935\ e^{-\left(\frac{M-1.27}{0.222}\right)^2} \quad for\ M > 0.8 \end{cases}$
$C(V_s)$	$1.35\ e^{-\left(\frac{V_s-3.84}{0.94}\right)^2} + 3.37\ e^{-\left(\frac{V_s-1.83}{3}\right)^2} - 1.86\ e^{-\left(\frac{V_s-1.227}{0.242}\right)^2} - 2.172\ e^{-\left(\frac{V_s-0.691}{0.45}\right)^2}$
$C(Epc)$	$\begin{cases} 1.78\ e^{-\left(\frac{Epc-1.355}{0.2}\right)^2} + 1.556\ e^{-\left(\frac{Epc-0.11}{0.57}\right)^2} + 0.48\ e^{-\left(\frac{Epc-0.673}{0.224}\right)^2} + 0.735\ e^{-\left(\frac{Epc-1.011}{0.226}\right)^2} \quad for\ Epc \le 1.24 \\ 1.9\ e^{-\left(\frac{Epc-3.304}{1.365}\right)^2} + 974.8\ e^{-\left(\frac{Epc+23.76}{9.77}\right)^2} \quad for\ Epc > 1.24 \end{cases}$

Table 19 Error distribution of predicted values relative to real values

Range of error	±5%	±10%	±15%	±17%	±18%	±19%
Number of data in this error range	13	26	42	45	46	48
Percentage to total data	27.10%	54.20%	87.50%	93.75%	95.83%	100%

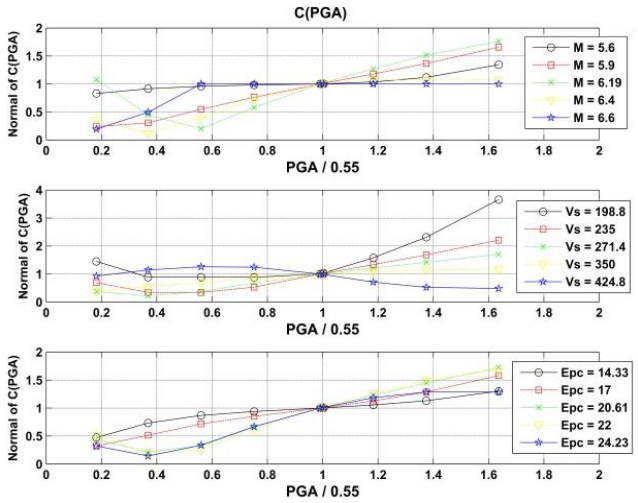

Fig. 9 C(PGA) with various values of "M", "V_s" and "Epc" – Single earthquakes with maximum PGA in 1st database

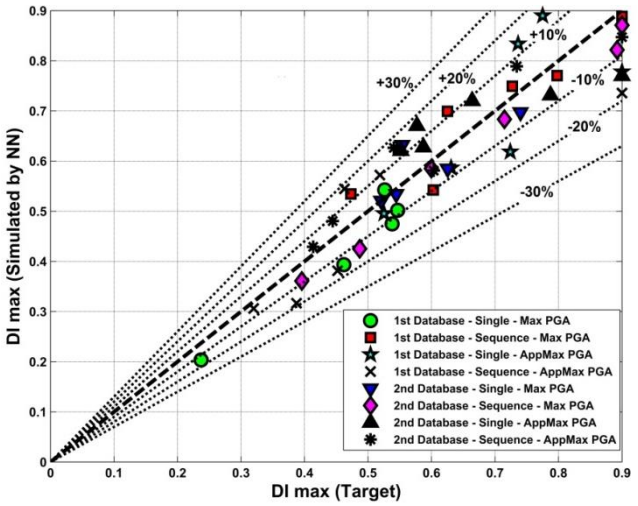

Fig. 10 Comparison of predicted values of maximum damage index versus real value according to Park-Ang damage index

consecutive earthquakes are listed in Tables 15-18. But all results of single and successive cases are reported in Fig. 10.

6. Comparison between simulated and real values of maximum damage

The proposed artificial neural network models are compared with the real values that introduced in the previous section. Fig. 10 shows the results in normal case base on record types and database. In this figure, horizontal and vertical axes are "the real value of maximum damage index based on Park-Ang damage index " and "the predicted value by neural network" respectively. The average error for the artificial neural network models–in both of single and consecutive earthquakes-for predicting the real results is equal to 9.3%.

To be more specific, more than 90% of the simulated results are within ±15% of the real values for artificial neural network models according to Table 19. This is an indication that the networks have learned to generalize the

unseen information well and reflects good precision in simulating. Moreover, concentrating on the Fig. 10, it can be seen that the values simulated by the artificial neural network model sets spread around the 45 degree line which implies neither over-estimation nor under-estimation.

7. Conclusions

In this investigation, large collections of experimental data from earthquake features and the resulting structural damage were gathered. Through the development of eight artificial neural networks (two databases with maximum and approximately maximum PGA in single and consecutive cases), the structural damage of reinforced concrete frames was related to some parameters such as, period of structures (T), Park-Ang damage index – as the results of nonlinear dynamic analysis in Opensees software (DI) – and some of earthquake features including PGA, magnitude (M), shear wave velocity at the station (V_s), epicentral distance (Epc) and time gap between consecutive earthquakes (T_g).

For each of the eight cases, after training the 400 neural networks with a different number of neurons in hidden layers, by considering the performance of the networks (MSE and *R*), one of the networks was selected for simulation which showed effective performance through training, testing, and validation. Also simulated values by the artificial neural network model sets spread around the 45 degree line which implied neither overestimation nor underestimation. Afterward, using the trained and validated networks, empirical design charts and correction equations are derived for calculation of maximum damage in regular reinforced concrete frames under single and consecutive earthquakes in the absence of the idealized network. On the other hand, equations which were derived predict the maximum damage index independently from the network.

The precision of the proposed equations was examined with real damage indexes (Park-Ang damage index) that showed good agreement.

So that the average error of the artificial neural network models for predicting the maximum damage results according to Park and Ang damage index (1985) under single and consecutive earthquakes, were lower than 10%, and more than 90% of the simulated results were within ±15% of the real values for artificial neural network models. The obtained results indicate that the networks were learned to generalize the information well.

References

Adnan, A., Tiong, P.L.Y., Ismail, R. and Shamsuddin, S.M. (2012), "Artificial neural network application for predicting seismic damage index of buildings in Malaysia", *Elec. J. Struct. Eng.*, **12**(1), 1-9.

ASCE/SEI **7**-05 (2005), Minimum Design Loads for Buildings and Other Structures, American Society of Civil Engineering.

Atkinson, G.M. (2009), "Earthquake time histories compatible with the 2005 NBCC uniform hazard spectrum", Dept. Earth Sciences, Univ. of Western Ontario, N6A 5B7, Can. J. Civil Engineering Wordcount.

Chen, H.M., Tsai, K.H., Qi, G.Z. and Yang, J.C.S. (1995), "Neural network for structural control", *J. Comput. Civil Eng.*, **9**(2), 168-176.

Dworakowski, Z., Ambrozinski, L., Dragan, K., Stepinski, T. and Uhl, T. (2014), "Voting neural network classifier for detection of fatigue damage in aircrafts", *7th European Workshop on Structural Health Monitoring*, Nantes, France.

El-Kordy, M.F., Chang, K.C. and Lee, G.C. (1993), "Neural networks trained by analytically simulated damage states", *J. Comput. Civil Eng.*, **7**(2), 130-145.

Garcia, J.R., Marin, M.V. and Gilmore, A.T. (2014), "Effect of seismic sequences in reinforced concrete frame buildings located in soft-soil sites", *Soil Dyn. Earthq. Eng.*, **63**, 56-68.

Guo, J., Wang, J.J., Li, Y., Zhao, W.G. and Du, .L. (2016), "Three dimentional extention for Park and Ang amage model", *Struct.*, ***7***, 184-194.

Hagan, M. (2014), *Neural Network Design*, 2nd Edition, eBook, Oklahoma State University Stillwater, Oklahoma.

Hajela, P. and Berke, L. (1991) "Neurobiological computational models in structural analysis and design", *Comput. Struct.*, **41**(4), 657-667.

Hancock, J., Bommer, J.J. and Stafford, P.J. (2008), "Numbers of scaled and matched accelerograms required for inelastic dynamic analyses", *Earthq. Eng. Struct. Dyn.*, **37**, 1585-1607.

Haselton, C.B.S., Taylor Lange, A.B. and Deierlein, G.G. (2007), "Beam-column element model calibrated for predicting flexural response leading to global collapse of RC frame buildings", Report No. PEER Report 2007/03, Berkeley Pacific Earthquake Engineering Research Center, College of Engineering, University of California.

Huang, W., Qian, J., Zhuang, B. and Fu, Q.S. (2012), "Damage assessment of RC frame structures under Mainshock-Aftershock Seismic Sequences", *Proceedings of the 15th World Conference on Earthquake Engineering (15WCEE)*, Portugal, Lisbon.

Kaveh, A., Kalateh-Ahani, M. and Fahimi-Farzam, M. (2014), "Damage-based optimization of large-scale steel structures", *Earthq. Struct.*, **7**(6), 1119-1139.

Leung, C.K., Ng, M.Y. and Luk, H.C. (2006), "Empirical approach for determining ultimate FRP strain in FRP-strengthened concrete beams", *J. Compos. Constr.*, **10**(2), 125-138.

McCulloch, W.S. and Pitts, W. (1943), "A logical calculus of the ideas immanent in nervous activity", *Bull. Math. Biophys.*, **5**(4), 115-133.

Mihai, M.A. (2013), "A theoretical review of the damage indices used to model the dynamic nonlinear behavior of reinforced concrete structures", *Buletinul Institutului Politehnic din lasi. Sectia Constructii, Arhitectura*, **59**(2), 109-119.

Nagae, T., Ghannoum, W.M., Kwon, J., Tahara, K., Fukuyama, K., Matsumori, T., Shiohara, H., Kabeyasawa, T., Kono, S., Nishiyama, M., Sause, R., Wallace, J.W. and Moehle, J.P. (2015), "Design implications of large-scale shake-table test on four-story reinforced concrete building", *ACI Struct. J.*, **112**(2), 135-146.

Opensees (2007), "Open system for earthquake engineering simulation", Pacific Earthquake Engineering Research Center, University of California, Berkeley.

Papaloizou, L., Polycarpou, P., Komodromos, P, Hatzigeorgiou, G.D. and Beskos, D.E. (2016), "Two-dimensional numerical investigation of the effects of multiple sequential earthquake excitations on ancient multidrum columns", *Earthq. Struct.*, **10**(3), 495-521.

Park, J. and Ang, A.H.S. (1985), "Mechanistic seismic damage model for reinforced concrete", *J. Struct. Eng.*, **III**(4), 722-739.

Park, Y.J., Reinhorn, A.M. and Kunnath, S.K. (1987), "IDARC: inelastic damage analysis of frame shear-wall-structures", Technical Report NCEER-87-0008, National Center for

Earthquake Engineering Research, State University of NewYork at Buffalo, NY.
PEER (2014), "Pacific earthquake engineering research center", University of California, Berkeley, Available at http://ngawest2.berkeley.edu/.
Tang, Z., Xie, X. and Wang, T. (2016), "Residual seismic performance of steel bridges under earthquake sequence", *Earthq. Struct.*, **11**(4), 649-664.
USGS (2015), "United states geological survey's earthquake hazards pProgram", Available at http://earthquake.usgs.gov.
Valles, R.E., Reinhorn, A.M., Kunnath, S.K., Li, C. and Madan, A. (1996), "IDARC version 4.0: a program for the inelastic damage analysis of reinforced concrete structures", Technical Report NCEER-96-0010, National Center for Earthquake Engineering Research, State University of New York at Buffalo.
Vamvatsikos, D. and Cornell, C.A. (2002), "Incremental dynamic analysis", *Earthq. Eng. Struct. Dyn.*, **31**, 491-514.
Xie, X., Lin, G., Duan, Y.F., Zhao, J.L. and Wang, R.Z. (2012), "Seismic damage of long span steel tower suspension bridge considering strong aftershocks", *Earthq. Struct.*, **3**(5), 767-781.
Zhai, C., Wen, W., Ji, D. and Li, S. (2015), "The influences of aftershocks on the constant damage inelastic displacement ratio", *Soil Dyn. Earthq. Eng.*, **79**, 186-189.
Zhai, C.H., Wen, W.P., Chen, Z., Li, S and Xie, L.L. (2013), "Damage spectra for the mainshock-aftershock sequence-type ground motions", *Soil Dyn. Earthq. Eng.*, **45**, 1-12.

CC